



ORIGINAL ARTICLE

Virus and bacterial removal ability of TiO₂ nanowire-based self-supported hybrid membranes



Mohammed Ahmed Shehab^{a,b}, Emma Szóri-Dorogházi^c, Szilvia Szabó^d,
Andrea Valsesia^e, Tanya Chauhan^a, Tamás Koós^f, Gábor Muránszky^g,
Tamás Szabó^h, Klara Hernadiⁱ, Zoltán Németh^{c,*}

^a Faculty of Materials Science and Engineering, University of Miskolc, H-3515 Miskolc, Hungary

^b Polymers and Petrochemicals Engineering Department, Basrah University for Oil and Gas, 61004 Basrah, Iraq

^c Advanced Materials and Intelligent Technologies Higher Education and Industrial Cooperation Centre, University of Miskolc, H-3515 Miskolc, Hungary

^d Kisanalitika Laboratory Services Ltd., Sajóbáony H-3792, Hungary

^e European Commission, Joint Research Centre (JRC), Ispra, Italy

^f Institute of Energy and Quality Affairs, University of Miskolc, H-3515 Miskolc, Hungary

^g Institute of Chemistry, University of Miskolc, H-3515 Miskolc, Hungary

^h Institute of Ceramics and Polymer Engineering, University of Miskolc, H-3515 Miskolc, Hungary

ⁱ Institute of Physical Metallurgy, Metal Forming and Nanotechnology, University of Miskolc, 3515 Miskolc-Egyetemváros, Hungary

Received 13 July 2022; accepted 3 November 2022

Available online 8 November 2022

KEYWORDS

Hybrid membrane;
TiO₂-based nanocomposites;
Micro CT;
E. coli removal;
MS2 removal

Abstract Development and application of hybrid membranes containing multi-component materials are increasing day by day in the fields of environmental protection and water treatment. In this research, the efficiency of titania nanowire (TiO₂ NW)-based self-supported hybrid membranes was investigated in the removal of *Escherichia coli* (*E. coli*) bacteria and MS2 bacteriophages from contaminated water mimicking the microorganism suspension. Furthermore, toxicology tests on the as-prepared membranes were also performed. TiO₂ NWs were coated with iron(III) oxide (Fe₂O₃) and copper(II) oxide (CuO) nanoparticles, respectively, and cellulose was used as reinforcement material. It was found that, the functionalisation strongly affected the MS2 removal ability of as-prepared membranes, which can be due to the electrostatic interactions between the surface of hybrid membrane and the bacteriophages. The most efficient removal (greater than or equal to 99.99%) was obtained with the TiO₂ NW-CuO-cellulose membrane at pH 7.0. The fabricated hybrid membranes were characterized by micro computed tomography (μCT), Raman spec-

* Corresponding author.

E-mail address: kemnemet@uni-miskolc.hu (Z. Németh).

Peer review under responsibility of King Saud University.



troscopy, Fourier transform infrared spectroscopy (FT-IR), dynamic light scattering (DLS), contact angle measurement and inductively coupled optical emission spectrometry (ICP-OES) techniques. This study shows a simple route of the usage of novel and effective inorganic nanowire-based hybrid membranes for bacteria and virus removal, providing new pathways in the field of water filtration technologies.

© 2022 The Author(s). Published by Elsevier B.V. on behalf of King Saud University. This is an open access article under the CC BY-NC-ND license (<http://creativecommons.org/licenses/by-nc-nd/4.0/>).

1. Introduction

As industrialization and population increasing continuously, the world faces an increasingly severe environmental pollution problem (N. Yerli-Soylu et al., 2022). The quality of available water is deteriorating due to the large amounts of contaminants discharged into water resources from factories and other human activities. One of the critical contaminants of water are micro pollutants (V. Manikandan et al., 2021) which include biological contaminants such as bacteria and viruses (B. M. Chabalala et al., 2021). Due to the tremendous adaptability of microorganisms to antibiotics and other antimicrobial agents, the effective removal of bacteria and viruses for industries like food processing or drinking water treatment has long been a significant challenge (P. Hajipour et al., 2021). Several efficient technologies have been developed and implemented to purify water, including photocatalysis (G. S. Sree et al., 2020), adsorption (S. Yuan et al., 2015), chemical precipitation (X. J. Wang et al., 2006), and membrane filtration (B. El Mrabate et al., 2021; M. A. Shehab et al., 2022).

Membrane filtration is a standard method for removing water pollutants from the environment because it is an energy-efficient method even at low levels of water pollutants (L. E. Mofokeng et al., 2022). The disadvantage of membrane filtration is that the process generates sludge which is difficult and expensive to dispose of. One of the possible solutions to overcome this negative phenomenon is to combine membrane filtration process with advantages of nanomaterials and photocatalytic materials. Some recently published paper summarized the progress of nanomaterial-modified membranes for wastewater treatment applications (A. Nain et al., 2022). Furthermore, recently published works show a growing interest in employing nanomaterials and nanostructured coatings to fight viruses, outside and inside the host (M. H. Dahanayake et al.; 2022).

Photocatalytic membrane processes can decompose pollutants in feed solutions by producing reactive oxygen species in the presence of UV light, thereby preventing the formation of a cake layer from the contaminant molecules on the membrane surface by degrading traces of contaminants attached to the surface (E. K. Tetteh et al., 2021). Thanks to the advancement of nanotechnology, it is now possible to use promising nanoparticles as antimicrobial/antibacterial agents. Interest in metal and metal oxide nanoparticles such as titanium, iron, and copper oxides has increased due to their low cost, non-toxicity, controllable characteristics (P. Hajipour et al., 2021).

Titanium dioxide (TiO_2) is one of the best photocatalysts known for photodegradation of organic pollutants, photo-induced bacterial and viral disinfection, and self-cleaning properties (J. Prakash et al., 2022). However, TiO_2 has a wide bandgap (3.2 eV) that limits its light absorption to UV light. One of the most promising methods to solve this problem is to decorate titania with a narrow band gap semiconductor (S. Zhang et al., 2020; B. Sharma et al., 2018).

Many researchers have demonstrated that the presence of metal oxides and bio-organic materials can improve the photocatalytic activity of titanium dioxide. P. Maheswari et al. prepared and evaluated the antibacterial and anticancer activities of pure and modified TiO_2 . The results show that TiO_2 modified with bio-organic materials has higher efficiency on anticancer and antibacterial properties than pure TiO_2 nanoparticles (P. Maheswari et al., 2020). E. Jeong et al. prepared Ni/ TiO_2 composite using a photodeposition method and investigated its antibacterial efficiency against *E. coli* and MS2 bacteriophage. It

was found that the composite has higher antibacterial properties than the pristine TiO_2 (E. Jeong et al., 2021). A. A. Sherwani et al. prepared Ag/ TiO_2 nanocomposite and evaluated its antibacterial activity toward *Staphylococcus aureus* (Gram-positive) and *Escherichia coli* (Gram-negative) bacteria. The results exhibited suitable antibacterial activities against both types of bacteria (A. A. Sherwani et al., 2021). E. Horvath et al. developed a photocatalytic-based nanocomposite filter based on TiO_2 nanowires and carbon nanotubes for water purification. It was found that photocatalytically generated reactive oxygen species (ROS) on the surface of the TiO_2 NWs/CNTs-based filter material under exposure to sunlight contribute to an efficient removal of a broad range of organic compounds and infective microbes (E. Horvath et al.; 2022).

G. Rao et al. synthesized silver (Ag) and copper (Cu)-loaded TiO_2 nanowire membrane and investigated their effectiveness in inactivating MS2 bacteriophage and *E. coli*. The Cu-Ag- TiO_2 membrane demonstrated more significant photo-activated bactericidal and virucidal activity than the TiO_2 , Ag- TiO_2 , and Cu- TiO_2 membranes under dark and UV light illumination (G. Rao et al., 2016).

Copper(II) oxide (CuO), one of the most readily available and inexpensive transition metal oxide, has significant potential to produce heterojunction areas when combined with TiO_2 . Due to its narrow band gap, CuO has been utilized in numerous applications, including photocatalytic removal of organic pollutants, an excellent antibacterial agent, and catalytic material. Moreover, the nontoxicity of this oxide is an essential feature (N. Sreeju et al., 2017). TiO_2 /CuO heterojunction composite photocatalysts have high photocatalytic and antibacterial properties (L. Gnanasekaran et al., 2021).

Iron(III) oxide (Fe_2O_3) nanoparticles have increasingly gained attention in photocatalytic decontamination due to their low cost, non-toxicity, large surface area, and particularly strong absorption in the visible light region (C. N. C. Hitam and A. A. Jalil, 2020). Iron oxide species with wider bandgaps, such as Fe_2O_3 (bandgap 2.3 eV), are more efficient for separating photo-induced charge carriers in heterojunctions than Fe_3O_4 with a narrow bandgap (0.1 eV). At ambient temperature, however, Fe_2O_3 is chemically more stable than Fe_3O_4 , which can be oxidized in the presence of oxygen. From this perspective, it is fair to assume that incorporating Fe_2O_3 nanoparticles into TiO_2 will considerably improve charge carrier separation in Fe_2O_3 - TiO_2 heterojunctions. The magnetic property of Fe_2O_3 is an important feature easier helps to recycle and regenerate, which utilizes a sustainable material for future applications (Q. Tao et al., 2020). R.T. Rasheed et al. prepared some inorganic metal oxides such as titanium dioxide (TiO_2), iron(III) oxide (Fe_2O_3), indium oxide (In_2O_3), and three composite nanopowders (TiO_2 - Fe_2O_3 , TiO_2 - In_2O_3 , and TiO_2 - Fe_2O_3 - In_2O_3) at (1:1, 1:1 and 1:1:1) mole ratios, respectively, using hydrothermal technique. Then investigate their antibacterial activity with two types of bacteria Gram-negative (*Escherichia coli*) and Gram-positive (*Staphylococcus aureus*). The results show that the composites have higher antibacterial activity than the pure nanopowders (R.T. Rasheed et al., 2019).

These days, the importance of selective removal of contaminants by membranes is increasing continuously in the field of water purification and environmental protection. In this regard S. Jahankhah et al. developed Fe_3O_4 /polydopamine (PDA)/Ag as adsorptive membrane by phase inversion method and investigate the filtration efficiency and adsorption of binary mixture Rhodamine B (RhB) and Auramine O

(AO) (S. Jahankhah et al.; 2022). In another study, in order to improve the filtration performance in-situ polymerization process was applied to prepare novel composite of Fe₃O₄/molecularly imprinted resorcinol-formaldehyde-melamine resin (Fe₃O₄/MIRFMR) (S. Jahankhah et al.; 2021). Resorcinol as functional monomers with multiple hydrophilic groups were used for selective removal of Rhodamine B (RhB) as target molecule. Based on the results it was found that the produced membrane could be an effective and selective option for wastewater treatment.

As it is well known, cellulose is one of the most abundant biopolymer. The abundance and unique structure makes it a remarkable material source for renewability, biodegradability, and biocompatibility. Moreover, its high number of hydroxyl groups results in large hydrogen bond networks, making it insoluble in most solvents. Consequently, it has recently been investigated in numerous advanced environmental and membrane technology applications, such as water and waste water treatment (Y. Li et al., 2018; S. Rashki et al., 2021).

Due to its specific chemical structure and properties, porosity, hydrophilicity, it is able to store a large amount of water, and efficiently transport oxygen and nutrients throughout, cellulose as support material for hybrid membranes is suitable to bacterial colonization and microorganism development. Furthermore, the cellulose and its derivate suitable for energy and environmental applications as well (P. Sherin et al.; 2022). For this reason, cellulose provides the ideal environment for bacterial growth. To overcome this problem, cellulose modification with antibacterial materials is widely investigated (B. El Mrabate et al., 2021). M. V. Arularasu et al. synthesized cellulose/TiO₂ nanocomposite using the precipitation method and investigated its antibacterial activity against *Staphylococcus aureus* and *Escherichia coli*. The result shows excellent antibacterial activity against tested *S. aureus* and *E. coli* bacteria (M. V. Arularasu et al., 2020). Cellulose fibres decorated with varying TiO₂ contents from 1 to 10 wt% nanoparticles were synthesized by I. Chauhan and P. Mohanty using a one-step hydrothermal process. The resultant composites contained 3.5 to 10 wt% of TiO₂ have good photocatalytic and antibacterial activity compared to pure cellulose (I. Chauhan and P. Mohanty, 2015). B. El Mrabate et al. successfully prepared and characterized cellulose reinforced hybrid membranes (B. El Mrabate et al., 2020) and presented their photocatalytic properties and bacterial removal efficiency against *E. coli* bacteria (B. El Mrabate et al., 2021).

The main objectives of this study were to characterize the TiO₂ NW-based membranes, to quantify the efficiency of the hybrid membranes by removing *E. coli* and MS2 bacteriophages from aqueous solutions, and to compare the performance of the different filters. One of our recent study has already showed the usage of TiO₂ NW-Fe₂O₃-cellulose and TiO₂ NW-CuO-cellulose hybrid membranes as a promising candidate in methylene blue MB removal and photodegradation (M. A. Shehab et al., 2022) and here we present the removal ability of these novel hybrid membranes against the *E. coli* and MS2. The unique hybrid membranes presented in this study could be ideal candidates water treatment and cleaning technologies.

2. Experimental

2.1. Materials

Titanium dioxide (TiO₂) (P25) with an average diameter of 21 nm, ammonium hydroxide (NH₄OH, 25 %) and sodium hydroxide (NaOH) was purchased from Sigma Aldrich (Hungary). The potassium hydroxide (KOH) was purchased from Thomasker Co., (Hungary). Iron chloride hexahydrate (FeCl₃·6H₂O) was purchased from Scharlab, (Hungary). Hydrochloric acid (HCl, 37 %), copper (II) acetate monohydrate (Cu(OOCC₃H₇)₂·H₂O) was ordered from VWR Chemicals (Hungary). Cellulose micro wires originating from the DIPA ltd (Hungary). Polyvinylidene (PVDF) filter membrane with a

diameter of 47 mm and the pore size of 0.1 μm (Durapore-VVLP04700) was used to produce the hybrid membranes.

Bacteriological agar, D-glucose, and sodium dihydrogen phosphate dihydrate (NaH₂PO₄·2H₂O) were purchased from Simga-Aldrich (Switzerland). Calcium chloride dihydrate (CaCl₂·2H₂O), microbiology yeast extract and glycerol were provided by Merck Eurolab (Switzerland). Streptomycin was purchased from AppliChem PanReac (Germany). Tryptone (Difco 0123) and sodium chloride (NaCl) were purchased from Becton Dickinson and VWR International (Switzerland), respectively. *Escherichia coli* DH5α (SZMC 21399) Gram-negative strain was used for filtration test as a model organism (this bacterial strain was gifted from the Department of Microbiology, Faculty of Science and Informatics, University of Szeged). *Escherichia coli* (Migula 1895) Castellani and Chalmers 1919 (DSM No.: 5695) colonies were used as host cells for MS2 bacteriophage multiplication (DSM No.: 13767). Dry *E. coli* pellets and the MS2 phage suspension were purchased from DSMZ (Braunschweig, Germany).

2.2. Preparation of TiO₂ NW-based hybrid membranes

In our earlier manuscript, the preparation and investigation of TiO₂ NW, the TiO₂ NW-Fe₂O₃ and TiO₂ NW-CuO nanocomposite additives (M. A. Shehab et al., 2022) were shown. Briefly, solvothermal process was used for the preparation of TiO₂ NW, and impregnation technique was applied to produce the inorganic composite additives such as TiO₂ NW-Fe₂O₃ and TiO₂ NW-CuO in both cases.

For the synthesis of hybrid membranes, firstly, the TiO₂ NW-Fe₂O₃ and TiO₂ NW-CuO nanocomposites were prepared. The calculated amount of FeCl₃·6H₂O and of (Cu(CH₃COO)₂·H₂O) precursors was dissolved in 100 mL of distilled water and 100 mL of EtOH respectively, to obtain a homogeneous solution. In the next step, TiO₂ NWs was added to the solutions and stirred for 1 h, then transferred to autoclave. The products obtained was washed to adjust the pH 7, and then calcinated for 2 h at 500 °C using a static furnace. The load of the Fe₂O₃ and CuO nanoparticles in the final nanocomposites was 5 w/w % each case.

To prepare the TiO₂ NW-Fe₂O₃-cellulose and TiO₂ NW-CuO-cellulose membranes, 0.2 g of the above-prepared composites was dipped into 100 mL of distilled water and EtOH, respectively for 1 h. Finally, 5 g of cellulose (1 w/w%) was added to the solution for another 1 h. Hybrid membranes were produced by vacuum filtration using PVDF membrane (total mass of 250 mg/membrane), then it was dried in a furnace for 30 min at 40 °C (M. A. Shehab et al., 2022).

2.3. Bacterial filtration efficiency (BFE) tests

For bacterial filtration efficiency tests, tenfold serial dilution was made from the initial starter culture in 30 mL Lysogeny Broth (LB) medium. The colony forming unit (cfu) concentration of the sixth tenfold dilution was $1.21 \pm 0.24 \times 10^3$ cfu/mL determined by the colony counting method. This suspension was used for the filtration experiment providing a countable number of colonies on the agar plate. Before each filtration, $3 \times 100 \mu\text{L}$ sample was evenly spread on the top of LB agar plate to check the initial colony forming unit concentration (CFU0). The filtration was performed using glass vacuum fil-

tration device (Sartorius Stedim Biotech 16306–25 mm) without vacuum pump, applying gravity driven filtration. After filtration $3 \times 100 \mu\text{L}$ sample was also taken from the filtrated suspension to determine the number of the colony forming units of the filtrate (CFUf) and then to derive BFE% values using the following formula:

$$\text{BFE}\% = \frac{\text{CFU}_0 - \text{CFU}_f}{\text{CFU}_0} \cdot 100\%$$

2.4. Virus filtration efficiency tests

The required media for bacteria and MS2 growth and filtration (such as antibiotic solution, broth, virus dilution buffer, hard and soft agar) were produced as offered by B.M. Pecson et al. (B. M. Pecson et al., 2009). MS2 was replicated using its host *Escherichia coli* strain and subsequently purified and concentrated in different steps, according to the protocol provided by DSMZ. Because of the sensitive nature of MS2 bacteriophages, the amount of plaque forming units (PFUs) in a suspension had to be determined from time to time. The initial stock of purified MS2 had the concentration of 7.6×10^7 PFU/mL. For further usage, the initial stock was diluted in virus dilution buffer (VDB). Hence, the detection limit of ~ 4 LRV (Log Reduction Value) or 99.99 % was determined by the phage enumeration that used a maximum sample volume of 2 mL. VDB was prepared using $\text{NaH}_2\text{PO}_4 \cdot 2\text{H}_2\text{O}$, NaCl and water. The pH (pH = 7.0) was adjusted by adding drops of 0.1 M NaOH solution. Room temperature (23 °C) was maintained throughout the virus filtration experiments. The concentration of the MS2 bacteriophages was determined after the incubation. Each enumeration of MS2 samples was performed twice, and each condition was tested three times.

Filtration experiments, the as-prepared hybrid membranes were placed into a 200 mL glass funnel with a porous glass insert at the bottom. During the experiments so-called gravity driven filtration was applied, consequently vacuum suction was not used to enhance the flux of the filtered liquid. A control experiment was also performed without a filter to investigate the influence of the equipment on the retention of the bacteriophages, given that the system is porous. 30 mL of the virus dilution buffer was infected with the calculated volume of bacteriophage stock to reach the active phage concentration of 10 PFU/mL. This allowed the investigation of retention of up to 2 magnitudes (2 Log). Separate experiments were performed both with membranes containing TiO_2 NW- Fe_2O_3 and TiO_2 NW-CuO nanocomposites. One millilitre of the filtered liquid was collected after each filtration and used to infect *E. coli* for virus enumeration. Filtration experiments were performed at pH values 7.0 to simulate real-life situations.

2.5. Toxicological tests

Toxicology test was done by the Kisanalitika Kft. (Sajóbáony - Hungary). Fish tests can be used to assess the environmental risk of surface water or to determine the toxic effects of pollution. Acute toxicity is a detectable adverse effect in an organism within a short period of time (within days) after exposure to a substance. In this study, acute toxicity is expressed as the lethal concentration 50 (LC50), i.e. the concentration of the

toxic material in water that causes death in 50 % of the test fish group within given period of time. A static test was used, so the test solution does not flow and the solutions remain unchanged throughout the experiments. In our case zebrafish (*Danio rerio*) were used to perform the tests. The fish must be in good health and free from any visible physical defects. Water toxicity testing was performed using a dilution series, using the water from the fish aquarium as dilution water, which also serves as the water for the control test group. The dilution water in the aquarium was aerated and its oxygen and pH were checked regularly. The test groups were placed in 500 mL of 24-hour soaking water of hybrid membranes or in water filtered also using the tested hybrid membranes. Each test group contained 5 fishes. Fishes were exposed to the test substance added to the water, over the concentration range tested, for a period of 48 h. Fish mortality was recorded at specified intervals, in this case after 2 h, 24 h and 48 h.

2.6. Characterization

The surface morphology and the three-dimensional architecture of hybrid membranes was characterized using YXLON FF35 dual-beam X-ray micro computed tomography equipment (CT) (microfocus X-ray tube, transmission beam, acceleration voltage: 50 kV).

Raman spectroscopy measurements were carried out using a high-resolution Raman spectrometer (Nicolet Almega XR, Thermo Electron Corporation, Waltham, MA, USA) equipped with a 532 nm Nd:YAG laser (50 mW).

Furthermore, our recently published paper presented a wide range of characterization of the as-prepared membranes, such as transmission electron microscopy (TEM), scanning electron microscopy (SEM), X-ray powder diffraction (XRD), specific surface area measurement (BET), etc., and their photocatalytic properties in the decomposition of against methylene blue organic dye (M. A. Shehab et al., 2022).

Electrophoretic measurement was performed by dynamic light scattering (DLS) (ZetaSizer NS-Malvern, UK) device. The measurement is based on the combination of laser Doppler velocimetry and phase analysis of light scattering (PALS) in Malvern's M3-PALS technique.

Inductively coupled optical emission spectrometry (ICP-OES) measurements were performed in a Varian 720 ES ICP-OES device to determine the amount of Cu and Fe dissolved during the filtration experiments.

The FTIR spectra were recorded on a Bio-Rad Digilab Division FTS65A/896 FT-IR spectrometer equipped with a DTGS detector and a Ge/KBr beamsplitter, between 4000 and 400 cm^{-1} , at 4 cm^{-1} optical resolution. A Harrick's Meridian® SplitPea Single Reflection Diamond ATR accessory was used, so no sample preparation was required. The spectrometer was controlled by Win IR Pro v. 3.3 (Bio-Rad Digilab Division) software, and the spectra were analyzed using GRAMS/AI v. 7.0 (Thermo Galactic) software.

3. Results and discussion

3.1. CT, Raman and FT-IR spectroscopy analysis

In our recently published study (M. A. Shehab et al., 2022) TEM and SEM analysis was performed in case of both TiO_2

NW-based composite additives and the hybrid membranes. It was found that the electron microscopy results showed properly the structure of as-prepared nanocomposite additives and the surface properties of hybrid membranes, although these measurements were did not provided information about the 3D structure of the hybrid membranes. Furthermore, there are some other limitations of the usage of the electron microscopy techniques in the field of membrane technology, such as the small size of the investigated area. In order to gain information about the homogeneity and the 3D morphology of the whole hybrid membrane structure, micro CT analysis was performed. Fig. 1 shows the 3D cross section analysis of TiO₂ NW-Fe₂O₃-cellulose (Fig. 1 a, b) and TiO₂ NW-CuO-cellulose (Fig. 1 c, d) membranes.

As can be seen in Fig. 1, no significant different was observed in the membrane structures. In both types of hybrid membrane, the brighter shapes represent the presence of cellulose, while the grey fibrous material was originating from the TiO₂ NW-Fe₂O₃ (Fig. 1 a, b) and TiO₂ NW-CuO (Fig. 1 c, d) nanocomposite additives. It was found, that in good

approximation homogeneous distribution of the nanocomposite additives and cellulose in the hybrid membrane structure was formed.

The material volume values of the hybrid membranes were also determined in the full 3D extension as can be seen in Table 1. There was no difference between the measured volume of materials, it was 0.33 mm³ in both cases. Furthermore, the obtained percentage by volume of materials values were also rather similar, the difference between the values was only 0.5 %. Based on the results obtained, it can be concluded that the 3D structure of the membranes produced is practically identical, so that the differences observed in the *E. coli* and MS2 filtration experiments are certainly due to differences in the material quality of the membranes and not to morphological differences.

In order to prove the chemical interaction between cellulose and TiO₂ NW-based nanocomposite additives, Raman spectroscopy analyses were recorded. Fig. 2a and b illustrates the Raman spectra of TiO₂ NW-CuO and TiO₂ NW-Fe₂O₃ nanocomposites (black curves), the pristine cellulose (red

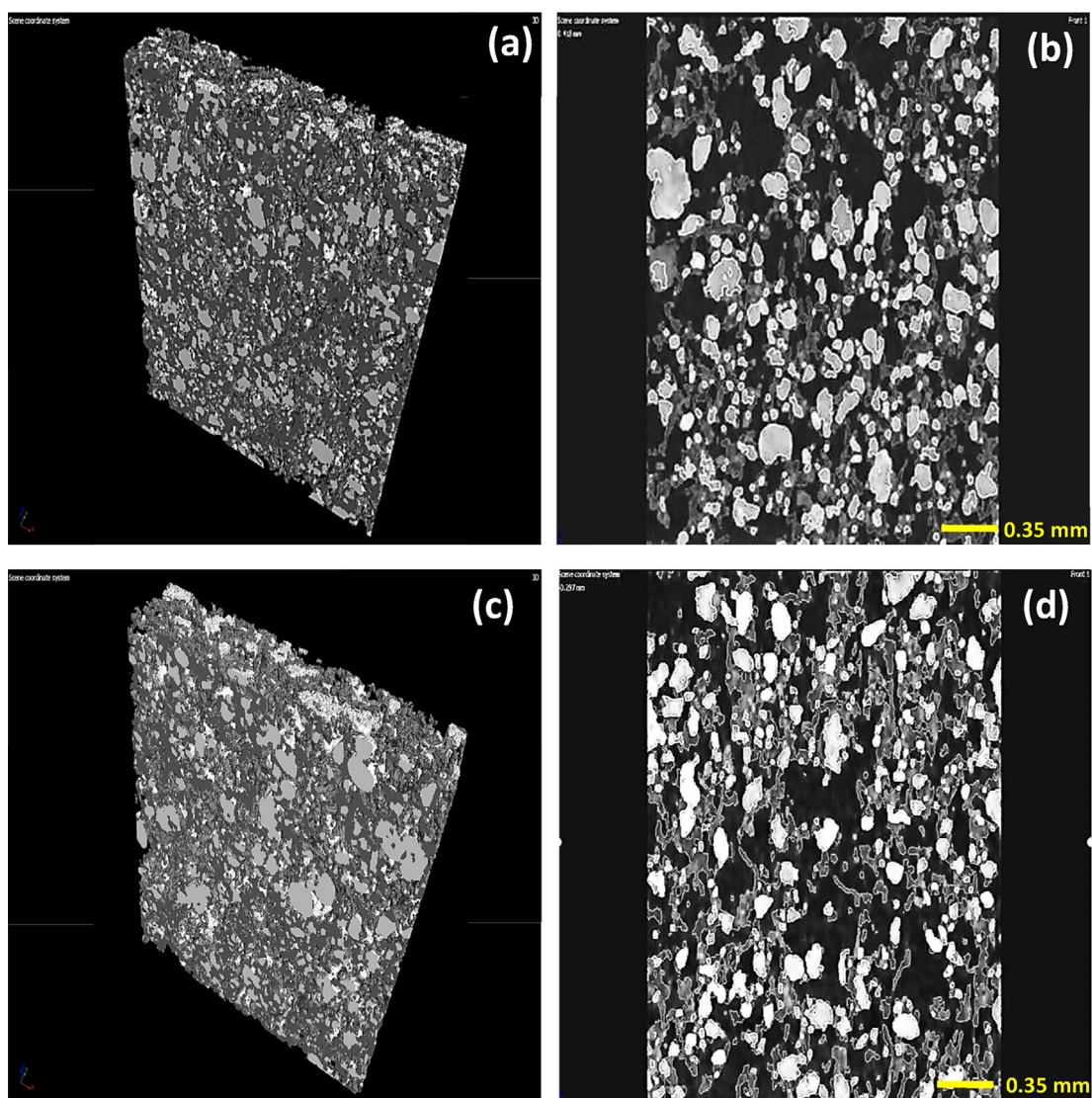


Fig. 1 3D CT cross section analysis of TiO₂ NW-Fe₂O₃-cellulose (a, b) and TiO₂ NW-CuO-cellulose (c, d) hybrid membranes.

Table 1 Material volume values of the hybrid membranes.

Sample	Volume of material (mm ³)	Percentage by volume of material (%)
TiO ₂ NWs-Fe ₂ O ₃ -cellulose	0.33	45.6
TiO ₂ NWs-CuO-cellulose	0.33	46.1

curves) and the as-prepared TiO₂ NW-CuO-cellulose and TiO₂ NW-Fe₂O₃-cellulose hybrid membranes (blue curves), respectively.

Raman spectra in Fig. 2a show three peaks at 143, 412, and 638 cm⁻¹ corresponding to the E_g (144 cm⁻¹), B_{1g} (399 cm⁻¹), and E_g (639 cm⁻¹) modes of anatase TiO₂ crystals, respectively (W. T. Pawlewicz et al., 1983), and peaks at 284 and 636 cm⁻¹ belonging to the A_g (296 cm⁻¹) and B_{2g} (636 cm⁻¹) modes of CuO crystals, respectively (T. Yu et al., 2004).

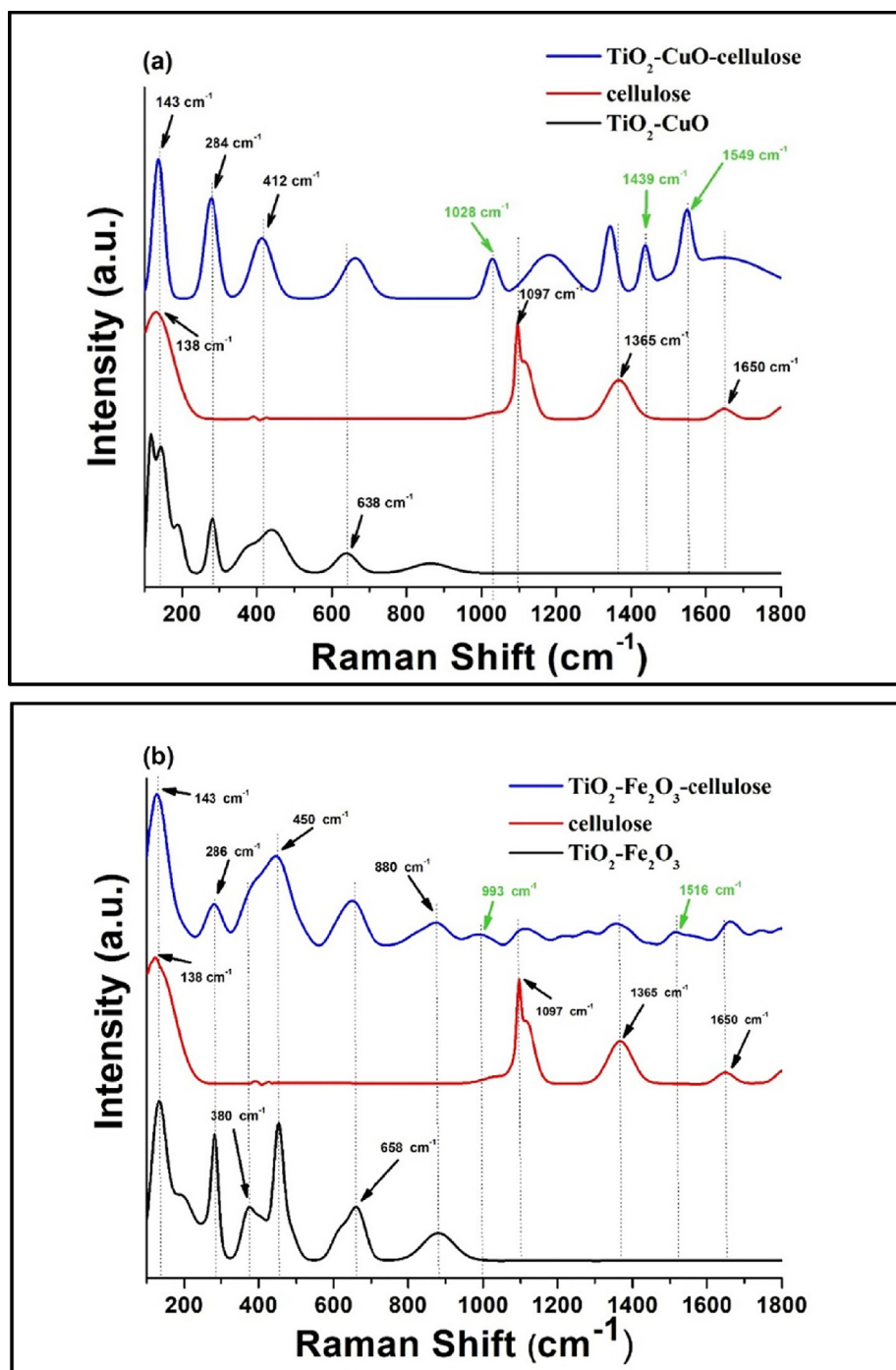


Fig. 2 Raman analysis of TiO₂-CuO-cellulose (a) and TiO₂-Fe₂O₃-cellulose (b) hybrid membranes.

The characteristic peaks of cellulose can be identified at 138, 1097, 1365 and 1650 cm^{-1} , as can be seen in Fig. 2 a red curve (K. Schenzel and S. Fischer, 2001). In Fig. 2 a blue curve shift in both the characteristic peaks of TiO₂-CuO nanocomposite and cellulose were observed in the spectrum of hybrid membrane. Moreover, as can be seen on the spectrum of the hybrid membrane new peaks appear at 1028, 1439 and 1549 cm^{-1} (marked by green colour in Fig. 2 a). It can be assumed that these bands originated from the interaction of the TiO₂-CuO nanocomposite and the oxygen containing surface functional groups of cellulose while there are no characteristic peaks of the nanocomposite and the cellulose in this region.

In the case of TiO₂-Fe₂O₃-cellulose hybrid membrane the Raman spectra in Fig. 2 b show three peaks at 143, 450 and 659 cm^{-1} corresponding to the E_g (144 cm^{-1}), B_{1g} (399 cm^{-1}), and E_g (639 cm^{-1}) modes of anatase TiO₂ crystals, respectively (W. T. Pawlewicz et al., 1983), and peaks at 286, 658 and 880 cm^{-1} belonging to the E_g (293, 613 and 814 cm^{-1}) modes of α -Fe₂O₃ crystals, respectively (H. Mansour et al.; 2020). Similarly, to the TiO₂-CuO-cellulose membrane (Fig. 2 a) the characteristic peaks of TiO₂-Fe₂O₃ nanocomposite and cellulose were shifted slightly in the spectrum of TiO₂-Fe₂O₃-cellulose hybrid membrane (Fig. 2 b blue curve). Furthermore, new peaks appear at 993 and 1516 cm^{-1} (marked by green colour in Fig. 2 b). These peaks can also be attributed to the interaction of the TiO₂-Fe₂O₃ nanocomposite and the oxygen containing surface functional groups of cellulose. The above-mentioned phenomena could be explained by the formation of non-covalent interactions, presumably hydrogen bonds, between the TiO₂-CuO, TiO₂-Fe₂O₃ nanocomposites and cellulose fibres, resulting in band shifting and new characteristic peaks (B. El Mrabate et al., 2020).

For further characterization and to answer the question without doubt, that chemical bond formed between the membrane components, FT-IR analysis was performed. Beside the reference cellulose (black curve) and TiO₂ NW/cellulose (red curve), the IR spectra of the hybrid membranes (blue and brown curves) are shown in Fig. 3 in the range of 400 to 800 cm^{-1} . This low frequency range features mainly the metal-oxygen stretching vibrational bands. As can be seen the black curve the cellulose has five bands with an intensity at 434, 518, 557, 609 and 663 cm^{-1} , while the TiO₂ NW/cellulose composite has two bands with considerable intensity at 439 and 584 cm^{-1} . In the case of hybrid membranes, the above mentioned peaks slightly shifted - from 439 cm^{-1} to 440 and 442 cm^{-1} and from 584 cm^{-1} to 586 cm^{-1} -, presumably due to the chemical interaction between the CuO, Fe₂O₃ nanoparticles and TiO₂ NW. Furthermore, a new band can be observed in both the hybrid membranes spectra at 669 cm^{-1} (marked by green), which is assigned to the metal-oxygen stretching band due to the presence of interaction between the TiO₂ NW and CuO and Fe₂O₃ nanoparticles, since there are no characteristic bands of the pristine components in this region (O. P. Keabadile et al., 2020; A. Lassoued et al., 2017).

3.2. Zeta potential and ICP-OES measurements

Zeta potential (ζ) of the hybrid membranes and raw materials was measured at pH 7.0 and the results presented in Table 2. Prior to the experiments, the samples were dispersed in deion-

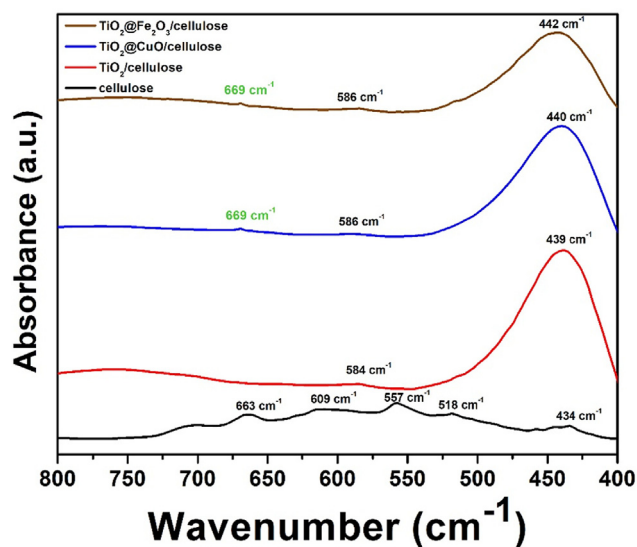


Fig. 3 FT-IR analysis of cellulose (black curve), TiO₂-cellulose (red curve), TiO₂-CuO-cellulose (blue curve) and TiO₂-Fe₂O₃-cellulose (brown curve).

Table 2 Zeta potential values of the pristine cellulose and the TiO₂ NWs-based membranes at pH 7.0.

Sample	Zeta (ζ) potential (mV)
cellulose	-32.2 ± 1.1
TiO ₂ NWs-cellulose	-27.9 ± 1.0
TiO ₂ NWs-Fe ₂ O ₃ -cellulose	-18.2 ± 0.5
TiO ₂ NWs-CuO-cellulose	-10.4 ± 0.3

ized water to reach the final concentration of 0.1 wt%. Each measurement was repeated three times.

By analyzing the ζ potential of cellulose, TiO₂ NWs-cellulose, and the hybrid membranes, we can conclude whether the efficiency of virus retention can be improved by the CuO and Fe₂O₃ nanoparticles adhered on the surface of TiO₂ NWs. The zeta potential of the neat cellulose is negative (-32.2 mV) whereas the hybrid membranes became more positively charged due to the functionalization (-18.2 and -10.4 mV). The surface treatment shifts the isoelectric point (IEP) towards higher values (the surface becomes more positively charged), consequently the filtration efficiency of MS2 could be also increasing, due to the electrostatic interaction between the surface of hybrid membranes and the bacteriophages. Since, the ζ potential of MS2 is approximately -30 mV (V.I. Syngouna and C.V. Chrysikopoulos, 2010), it is not expected a high virus retention value from the pure cellulose with a ζ potential of -32.2 mV.

In contrast to this, Fe₂O₃ and CuO nanoparticles have been shown to have positive ζ potential at pH 7.0 (M. Kosmulski, 2009). It can also be ascertained that the surface functionalization of TiO₂ NWs by applying CuO and Fe₂O₃ nanoparticles shifted the zeta potential values to less negative region in the case of hybrid membranes, as can be seen in Table 2. These findings mean that the electric properties of the surface of

Table 3 Determination of dissolved amount of Cu and Fe content by ICP-OES measurement.

Sample	Cu ($\mu\text{g/L}$)	Fe ($\mu\text{g/L}$)
TiO ₂ /Fe ₂ O ₃ /cellulose		57 \pm 0,0010
TiO ₂ /CuO/cellulose	46 \pm 0,0003	

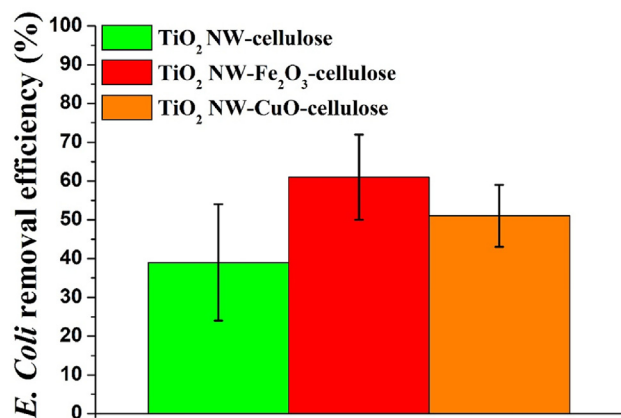


Fig. 4 *E. coli* removal efficiency (BFE%) of TiO₂ NW-based hybrid membranes.

TiO₂ NWs-based membranes are more favourable for the retention of MS2 bacteriophages.

Samples for inductively coupled optical emission spectrometry (ICP-OES) measurements have been prepared to determine the total dissolved Cu and Fe content by filtering deionized water of pH 7.0 through the membrane under the previously detailed experimental conditions. The results show in Table 3 that in each case the dissolved amount of metal ions less than the WHO limitations (World Health Organization, 2017) (Cu < 2 mg/L; Fe - no health-based guideline value is proposed for iron); thus, the dissolution of Cu and Fe during filtration does not overstep in extent the international guidelines. Furthermore, based on the values obtained, it is assumed that leaching not affects the results of *E. Coli* and MS2 filtration experiments.

3.3. *E. coli* filtration experiments results

Before the filtration tests began, control experiments were performed without applying the as-prepared hybrid membranes to investigate the possible adsorption on the membrane holder of the funnel. The *E. coli* removal efficiency values are shown in Fig. 4. In both cases, the membranes containing TiO₂ NW-based inorganic nanocomposite additives showed significantly higher *E. coli* removal (Fig. 4 red and orange columns) than membranes were build using only TiO₂ NW and cellulose without the usage of Fe₂O₃ and CuO nanoparticles (Fig. 4 green column). As can be seen the highest *E. coli* removal was achieved by the TiO₂ NW-Fe₂O₃-cellulose membrane with an efficiency of 61 % (Fig. 4 red column). Furthermore, the effectiveness of TiO₂ NW-CuO-cellulose membrane was increased (Fig. 4 orange column – 51 %) comparing with the pure TiO₂ NW-cellulose membrane (Fig. 4 green column – 39 %). Although, the removal efficiency of the pure cellulose membrane was also measured it was not presented in the Fig. 3, because of it was not feasible the gravity driven filtration with these membranes.

Based on the above-mentioned results, it was found that in terms of *E. coli* removal, the incorporation of TiO₂ NW-Fe₂O₃ and TiO₂ NW-CuO nanocomposites into the hybrid membrane structures provided increased bacteria removal efficiency. As can be seen in Fig. 4 the application of TiO₂ NW-based additives caused a significant improvement in the *E. coli* filtration efficiency in both cases. Consequently, the outstanding filtration performance of hybrid membranes indicates that the removal properties of the membranes are mainly attributed to the TiO₂ NW-Fe₂O₃ and TiO₂ NW-CuO nanocomposite additives.

3.4. MS2 filtration experiments results

The results of MS2 filtration experiments are presented in Figs. 5 and 6. It was found that both membranes were capable of retaining MS2 bacteriophages as model contaminants, but the efficiency of the membranes was significantly different.

As can be seen in Fig. 5 c and Fig. 6 orange column the CuO-coated TiO₂ NW-based membrane provided the most promising adsorption properties. While the TiO₂-CuO-cellulose membrane showed LRV of up to 2 at pH 7 (Fig. 5 c and Fig. 6 orange column), the LRVs of TiO₂-Fe₂O₃-

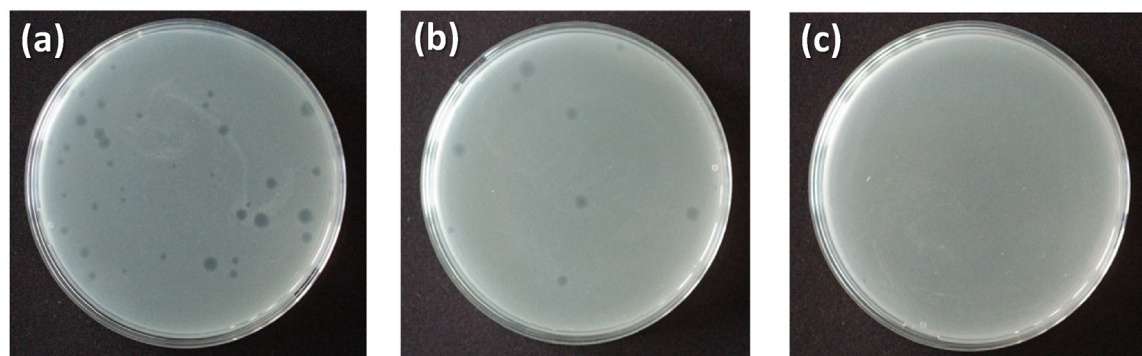


Fig. 5 MS2 enumeration plates of TiO₂-cellulose (a); TiO₂-Fe₂O₃-cellulose (b) and TiO₂-CuO-cellulose (c) membranes after filtration experiments, investigating 2 LRV value.

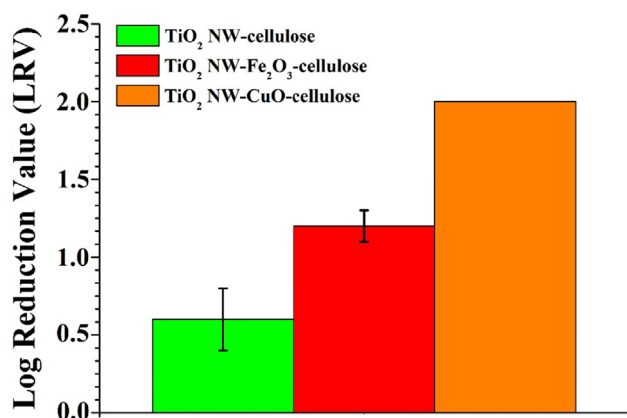


Fig. 6 MS2 retention of the TiO₂ NW-based hybrid membranes in gravity driven filtration.

Table 4 Toxicological results of hybrid membranes.

Sample	mortality after 2 h	mortality after 24 h	mortality after 48 h
TiO ₂ NWs/cellulose	none	none	none
TiO ₂ NWs-Fe ₂ O ₃ /cellulose	none	none	none
TiO ₂ NWs-CuO/cellulose	none	none	none

cellulose and TiO₂-cellulose membranes showed significantly lower virus retention capacity. In the case of TiO₂-Fe₂O₃-cellulose membrane (Fig. 5 b and Fig. 6 red column) the virus retention value was 1.2 LRV, while this value was only 0.6 LRV using TiO₂-cellulose membrane (Fig. 5 a and Fig. 6 green column). As it was previously published, during virus filtration not only the specific surface area but also the electrostatic force between the bacteriophages and the adsorbents are very significant parameters for virus rejection (Z. Németh et al., 2019). The enhanced virus retention value in the case of TiO₂-CuO-cellulose membrane can be explained by two main phenomena: the inactivation of virions by CuO nanoparticles and their surface adsorption by electrostatic force (L. Sellaoui et al., 2021).

3.5. Toxicology experiments results

The results of the toxicological tests are given in Table 4. After performing the tests, it was found that none of the membranes showed any toxic properties under the experimental set-up we used (1 membrane soaked in 500 mL dilution water or 500 mL of filtered water, respectively). None of the fish groups showed any mortality during the test period.

4. Conclusion

In this study, a successful attempt with TiO₂ nanowire-based hybrid membranes was showed in the field of removal of pathogens from water by gravity-driven filtration. The bacterial and virus retention ability against Gram-negative *E. coli* bacteria and MS2 bacteriophages of the novel TiO₂ nanowire-based hybrid membranes were studied, respectively.

Comparing inorganic components of nanocomposite materials, Fe₂O₃ decorated TiO₂ NW-based membranes showed somewhat higher *E. coli* removal value (61 %) than CuO decorated membranes (51 %), while the TiO₂ NW-CuO-cellulose samples presented outstanding efficiency in virus filtration experiment. Results revealed that the TiO₂ NW-CuO-cellulose membranes provide noteworthy virus retention capability and our results confirmed a virus retention of up to 2 Log (99.99 %). Probably due to the synergetic effect of TiO₂-CuO nanocomposite and cellulose matrix material, the as-prepared hybrid membranes could provide a possible solution for water cleaning, since TiO₂ could potentially increase adsorption efficacy of organic pollutants from water and also serve as high-surface-area support to the CuO nanoparticles as virus adsorbent. Hence, efficiency as “at least” LRV = 2 Log should indicate, since there were no more MS2 to be removed at the end of the experiment. Presumably, it can mean, that the MS2 removal efficiency of the TiO₂ NW-CuO-cellulose membrane can be even higher. Future experiments with higher initial virion concentrations are planned to judge the real LRV of the selected nanocomposite. The overall excellence performance of the TiO₂-CuO-cellulose hybrid membranes suggests that future development could be resulted a promising membrane material for the treatment of pathogens-contaminated water. In the near future, we would like to perform stability tests on the membranes after their optimization to larger water quantities, in order to provide alternatives for everyday water treatment applications. Besides, the regeneration and reusability of the as-prepared hybrid membranes by the involvement of environmental UV chamber is also planned.

Declaration of Competing Interest

The authors declare that they have no known competing financial interests or personal relationships that could have appeared to influence the work reported in this paper.

Acknowledgements

This research was funded by National Research, Development and Innovation Office (NRDI Fund), grant number 2020-2.1.1-ED-2020-00029, Hungary and the experimental data used in this research were generated through access to the JRC Nanobiotechnology Laboratory under the Framework of access to the Joint Research Centre Physical Research Infrastructures of the European Commission (Virimmo project, Research Infrastructure Access Agreement N° 36171/11). We would like to acknowledge to the Kisanalitika Laboratory Services Ltd. for the toxicology investigations and the DIPA Zrt. that provided for us the raw cellulose material. Zoltán Németh would like to thank the Hungarian Academy of Sciences Bolyai János Research Scholarship Program.

References

- Arularasua, M.V., Harbb, M., Sundaram, R., 2020. Synthesis and characterization of cellulose/TiO₂ nanocomposite: Evaluation of in vitro antibacterial and in silico molecular docking studies. *Carbohydr. Polymers* 249,. [https://doi.org/10.1016/j-carbpol.2020.116868](https://doi.org/10.1016/j.carbpol.2020.116868) 116868.
- Chabalala, B.M., Gumbi, N.N., Mamba, B.B., Al-Abri, M.Z., Nxumalo, E.N., 2021. Photocatalytic nanofiber membranes for the degradation of micropollutants and their antimicrobial activity: recent advances and future prospects. *Membranes* 11, 678. <https://doi.org/10.3390/membranes11090678>.
- Chauhan, I., Mohanty, P., 2015. In situ decoration of TiO₂ nanoparticles on the surface of cellulose fibers and study of their

- photocatalytic and antibacterial activities. *Cellulose* 22, 507–519. <https://doi.org/10.1007/s10570-014-0480-3>.
- Dahanayake, M.H., Athukorala, S.S., Jayasundera, A.C.A., 2022. Recent breakthroughs in nanostructured antiviral coating and filtration materials: a brief review. *RSC Adv.* 12, 16369.
- El Mrabate, B., Udayakumar, M., Csiszar, E., Kristaly, F., Lesko, M., Somlyai Sipos, L., Schabikowski, M., Nemeth, Z., 2020. Development of bacterial cellulose–ZnO–MWCNT hybrid membranes: a study of structural and mechanical properties. *R. Soc. Open Sci.* 7, <https://doi.org/10.1098/rsos.200592> 200592.
- El Mrabate, B., Szori-Doroghazi, E., Shehab, M.A., Chauhan, T., Muranszky, G., Sikora, E., Filep, A., Sharma, N., Nanai, L., Hernadi, K., Nemeth, Z., 2021. Widespread applicability of bacterial cellulose–ZnO–MWCNT hybrid membranes. *Arab. J. Chem.* 14, <https://doi.org/10.1016/j.arabjc.2021.103232> 103232.
- Gnanasekaran, L., Pachaiappan, R., Kumar, P.S., Hoang, T.K.A., Rajendran, S., Durgalakshmi, D., Soto-Moscoco, M., Cornejo-Ponce, L., Gracia, F., 2021. Visible light driven exotic p (CuO) - n (TiO₂) heterojunction for the photodegradation of 4-chlorophenol and antibacterial activity. *Environ. Pollut.* 287, <https://doi.org/10.1016/j.envpol.2021.117304> 117304.
- Hajipour, P., Eslami, A., Bahrami, A., Hosseini-Abari, A., Saber, F. Y., Mohammadi, R., Mehr, M.Y., 2021. Surface modification of TiO₂ nanoparticles with CuO for visible-light antibacterial applications and photocatalytic degradation of antibiotics. *Ceram. Inter.* 47 (23), 33875–33885. <https://doi.org/10.1016/j.ceramint.2021.08.300>.
- Hitam, C.N.C., Jalil, A.A., 2020. A review on exploration of Fe₂O₃ photocatalyst towards degradation of dyes and organic contaminants. *J. Environ. Management* 258, <https://doi.org/10.1016/j.jenvman.2019.110050> 110050.
- Horváth, E., Gabathuler, J., Bourdieu, G., Vidal-Revel, E., Muniz, M. B., Gaal, M., Grandjean, D., Breider, F., Rossi, L., Sienkiewicz, A., Forró, L., 2022. Solar water purification with photocatalytic nanocomposite filter based on TiO₂ nanowires and carbon nanotubes. *npj Clean. Water* 5 (1), 1–11. <https://doi.org/10.1038/s41545-022-00157-2>.
- Jahankhah, S., Sabzehmeidani, M.M., Ghaedi, M., Dashtian, K., Abbasi-Asl, H., 2021. Hydrophilic magnetic molecularly imprinted resin in PVDF membrane for efficient selective removal of dye. *J. Environ. Manag.* 300, <https://doi.org/10.1016/j.jenvman.2021.113707> 113707.
- Jahankhah, S., Sabzehmeidani, M.M., Ghaedi, M., Dashtian, K., Abbasi-Asl, H., 2022. Fabrication polyvinyl chloride mixed matrix membrane via embedding Fe₃O₄/polydopamine /Ag nanocomposite for water treatment. *Mat. Sci. Eng. B* 285, <https://doi.org/10.1016/j.mseb.2022.115935> 115935.
- Jeong, E., Park, H.Y., Lee, J., Kim, H.-E., Lee, C., Kim, E.J., Hong, S. W., 2021. Long-term and stable antimicrobial properties of immobilized Ni/TiO₂ nanocomposites against *Escherichia coli*, *Legionella thermalis*, and MS2 bacteriophage. *Environ. Res.* 194, <https://doi.org/10.1016/j.envres.2020.110657> 110657.
- Keabadile, O.P., Aremu, A.O., Elugoke, S.E., Fayemi, O.E., 2020. Green and traditional synthesis of copper oxide nanoparticles - comparative study. *Nanomaterials* 10 (12), 2502. <https://doi.org/10.3390/nano10122502>.
- Kosmulski, M. 2009. Surface charging and points of zero charge. *Surfactant Sci. Series* 145. 1st edition. CRC Press, Boca Raton. <https://doi.org/10.1201/9781420051896>.
- Lassoued, A., Dkhil, B., Gadri, A., Ammar, S., 2017. Control of the shape and size of iron oxide (α -Fe₂O₃) nanoparticles synthesized through the chemical precipitation method. *Results Phys.* 7, 3007–3015. <https://doi.org/10.1016/j.rinp.2017.07.066>.
- Li, Y., Tian, J., Yang, C., Hsiao, B.S., 2018. Nanocomposite film containing fibrous cellulose scaffold and Ag/TiO₂ nanoparticles and its antibacterial activity. *Polymers* 10, 1052. <https://doi.org/10.3390/polym10101052>.
- Maheswari, P., Ponnusamy, S., Harish, S., Ganesh, M.R., Hayakawa, Y., 2020. Hydrothermal synthesis of pure and bio modified TiO₂: characterization, evaluation of antibacterial activity against gram positive and gram negative bacteria and anticancer activity against KB oral cancer cell line. *Arab. J. Chem.* 13, 3484–3497. <https://doi.org/10.1016/j.arabjc.2018.11.020>.
- Manikandan, V., Mahadik, M.A., Hwang, I.S., Chae, W.-S., Ryu, J., Jang, J.S., 2021. Visible-light-active CuO_x-loaded Mo-BiVO₄ photocatalyst for inactivation of harmful bacteria (*Escherichia coli* and *Staphylococcus aureus*) and degradation of orange II dye. *ACS Omega* 6, 23901–23912. <https://doi.org/10.1021/acsomega.1c02879>.
- Mansour, H., Omri, K., Bargougui, R., Ammar, S., 2020. Novel α -Fe₂O₃/TiO₂ nanocomposites with enhanced photocatalytic activity. *Appl. Phys. A* 126, 151. <https://doi.org/10.1007/s00339-020-3320-3>.
- Mofokeng, L.E., Hlekelele, L., Moma, J., Tetana, Z.N., Chauke, V.P., 2022. Energy-efficient CuO/TiO₂@GCN cellulose acetate-based membrane for concurrent filtration and photodegradation of ketoprofen in drinking and groundwater. *Appl. Sci.* 12, 1649. <https://doi.org/10.3390/app12031649>.
- Nain, A., Sangili, A., Hu, S.-R., Chen, C.-H., Chen, Y.-L., Chang, H.-T., 2022. Recent progress in nanomaterial-functionalized membranes for removal of pollutants. *iScience* 25, (7). <https://doi.org/10.1016/j.isci.2022.104616> 104616.
- Németh, Z., Szekeres, G.P., Schabikowski, M., Schrantz, K., Traber, J., Pronk, W., Hernádi, K., Graule, T., 2019. Enhanced virus filtration in hybrid membranes with MWCNT nanocomposite. *Roy. Soc. Open Sci.* 6, <https://doi.org/10.1098/rsos.181294> 181294.
- Pawlewicz, W.T., Exarhos, G.J., Conaway, W.E., 1983. Structural characterization of TiO₂ optical coatings by Raman spectroscopy. *Appl. Opt.* 22 (12), 1837. <https://doi.org/10.1364/ao.22.001837>.
- Pecson, B.M., Martin, L.V., Kohn, T., 2009. Quantitative PCR for determining the infectivity of bacteriophage MS2 upon inactivation by heat, UV-B radiation, and singlet oxygen. *Appl. Environ. Microbiol.* 75, 5544–5554. <https://doi.org/10.1128/AEM.00425-09>.
- Prakash, J., Cho, J., Mishra, Y.K., 2022. Photocatalytic TiO₂ nanomaterials as potential antimicrobial and antiviral agents: scope against blocking the SARS-COV-2 spread. *Micro Nano Eng.* 14, <https://doi.org/10.1016/j.mne.2021.100100> 100100.
- Rao, G., Brastad, K.S., Zhang, Q., Robinson, R., He, Z., Li, Y., 2016. Enhanced disinfection of *Escherichia coli* and bacteriophage MS2 in water using a copper and silver loaded titanium dioxide nanowire membrane. *Front. Environ. Sci. Eng.* 10 (4), 11. <https://doi.org/10.1007/s11783-016-0854-x>.
- Rasheed, R.T., Mansoor, H.S., Qasim, B.H., 2019. Antibacterial activity of TiO₂ and TiO₂ composites nanopowders prepared by hydrothermal method. *Materials Research Express* 6, 0850a5. <https://doi.org/10.1088/2053-1591/ab2313>.
- Rashki, S., Shakour, N., Yousefi, Z., Rezaei, M., Homayoonfal, M., Khabazian, E., Atyabi, F., Aslanbeigi, F., Lapavandani, R.S., Mazaheri, S., Hamblin, M.R., Mirzaei, H., 2021. Cellulose-based nanofibril composite materials as a new approach to fight bacterial infections. *Front. Bioeng. Biotechnol.* 9, <https://doi.org/10.3389/fbioe.2021.732461> 732461.
- Schenzel, K., Fischer, S., 2001. NIR FT Raman spectroscopy - a rapid analytical tool for detecting the transformation of cellulose polymorphs. *Cellulose* 8, 49–57. <https://doi.org/10.1023/A:1016616920539>.
- Sellaoui, L., Badawi, M., Monari, A., Tatarchuk, T., Jemli, S., Dotto, G.L., Bonilla-Petriciolet, A., Chen, Z., 2021. Make it clean, make it safe: A review on virus elimination via adsorption. *Chem. Eng. J.* 412, <https://doi.org/10.1016/j.cej.2021.128682> 128682.
- Sharma, B., Boruah, P.K., Yadav, A., Das, M.R., 2018. TiO₂-Fe₂O₃ nanocomposite heterojunction for superior charge separation and the photocatalytic inactivation of pathogenic bacteria in water under direct sunlight irradiation. *J. Environ. Chem. Eng.* 6 (1), 134–145. <https://doi.org/10.1016/j.jece.2017.11.025>.

- Sharwani, A.A., Narayanan, K.B., Khan, M.E., Han, S.S., 2021. Sustainable fabrication of silver-titania nanocomposites using goji berry (*Lycium barbarum* L.) fruit extract and their photocatalytic and antibacterial applications. *Arab. J. Chem.* 14. <https://doi.org/10.1016/j.arabjc.2021.103456> 103456.
- Shehab, M.A., Sharma, N., Valsesia, A., Karacs, G., Kristály, F., Koós, T., Leskó, A.K., Nánai, L., Hernadi, K., Németh, Z., 2022. Preparation and photocatalytic performance of TiO₂ nanowire-based self-supported hybrid membranes. *Molecules* 27 (9), 2951. <https://doi.org/10.3390/molecules27092951>.
- Sherin, P., Lyczko, N., Gopakumar, D., Maria, H.J., Nzihou, A., Sabu, T., 2022. Nanocellulose and its derivative materials for energy and environmental applications. *J. Mater. Sci.* 57, 6835–6880.
- Sree, G.S., Botsa, S.M., Reddy, B.J.M., Ranjitha, K.V.B., 2020. Enhanced UV-Visible triggered photocatalytic degradation of brilliant green by reduced graphene oxide based NiO and CuO ternary nanocomposite and their antimicrobial activity. *Arab. J. Chem.* 13 (4), 5137–5150. <https://doi.org/10.1016/j.arabjc.2020.02.012>.
- Sreeju, N., Rufus, A., Philip, D., 2017. Studies on catalytic degradation of organic pollutants and anti-bacterial property using biosynthesized CuO nanostructures. *J. Mol. Liq.* 242, 690–700. <https://doi.org/10.1016/j.molliq.2017.07.077>.
- Syngouna, V.I., Chrysikopoulos, C.V., 2010. Interaction between Viruses and Clays in Static and Dynamic Batch Systems. *Environ. Sci. Technol.* 44 (12), 4539–4544. <https://doi.org/10.1021/es100107a>.
- Tao, Q., Huang, X., Bi, J., Wei, R., Xie, C., Zhou, Y., Yu, L., Hao, H., Wang, J., 2020. Aerobic oil-phase cyclic magnetic adsorption to synthesize 1D Fe₂O₃@TiO₂ nanotube composites for enhanced visible-light photocatalytic degradation. *Nanomaterials* 10, 1345. <https://doi.org/10.3390/nano10071345>.
- Tetteh, E.K., Rathilal, S., Asante-Sackey, D., Chollom, M.N., 2021. Prospects of synthesized magnetic TiO₂-based membranes for wastewater treatment: a review. *Materials* 14, 3524. <https://doi.org/10.3390/ma14133524>.
- Wang, X.J., Xia, S.Q., Chen, L., Zhao, J.F., Renault, N.J., Chovelon, J.M., 2006. Nutrients removal from municipal wastewater by chemical precipitation in a moving bed biofilm reactor. *Process Biochem.* 41 (4), 824–828. <https://doi.org/10.1016/j.procbio.2005.10.015>.
- World Health Organization, 2017. Guidelines for drinking-water quality. 4th ed. Geneva, pp. 242–244. <https://www.who.int/publications/i/item/9789241549950>.
- Yerli-Soylu, N., Akturk, A., Kabak, Ö., Erol-Taygun, M., Karbançoglu-Guler, F., Küçükbayrak, S., 2022. TiO₂ nanocomposite ceramics doped with silver nanoparticles for the photocatalytic degradation of methylene blue and antibacterial activity against *Escherichia coli*. *Eng. Sci. Technol. Inter J.* <https://doi.org/10.1016/j.jestech.2022.101175> 101175.
- Yu, T., Zhao, X., Shen, Z.X., Wu, Y.H., Su, W.H., 2004. Investigation of individual CuO nanorods by polarized micro-Raman scattering. *J. Cryst. Growth* 268 (3–4), 590–595. <https://doi.org/10.1016/j.jcrysgro.2004.04.097>.
- Yuan, S., Gu, J., Zheng, Y., Jiang, W., Liang, B., Pehkonen, S.O., 2015. Purification of phenol-contaminated water by adsorption with quaternized poly(dimethylaminopropyl methacrylamide)-grafted PVBC microspheres. *J. Mater. Chem. A* 3, 4620–4636. <https://doi.org/10.1039/C4TA06363E>.
- Zhang, S., Yi, J., Chen, J., Yin, Z., Tang, T., Wei, W., Cao, S., Xu, H., 2020. Spatially confined Fe₂O₃ in hierarchical SiO₂@TiO₂ hollow sphere exhibiting superior photocatalytic efficiency for degrading antibiotics. *Chem. Eng. Journal*, 122583. <https://doi.org/10.1016/j.cej.2019.122583>. 380.